Matrix-Assisted Biomimetic Assembly of Ferritin Core Analogues in Organosilica Sol−Gels

Mukti S. Rao,[†] Igor S. Dubenko,[‡] Sujoy Roy,[‡] Naushad Ali,[‡] and Bakul C. Dave*[,†]

Department of Chemistry and Biochemistry Department of Physics, Southern Illinois University Carbondale, Carbondale, Illinois 62901

Received August 31, 2000

Biological self-assembly of superparamagnetic iron−oxo cores in ferritin illustrates a unique example of matrix-assisted formation of magnetic nanomaterials[1] and artificial analogues of ferritin still remain an elusive goal. In this context, synthesis of iron oxide nanoparticles has been attempted by different methods.[2−8] However, a critical requirement in modeling the fundamental aspects of ferritin core assembly is direct chemical involvement of a template analogous to ferritin which uses coordinating residues from the protein shell for binding metal ions and directing their growth.[9,10] Herein, we describe a system containing nanoclusters of iron oxide—assembled in situ within the nanopores of an organosilica sol−gel[11]—that is capable of mimicking all the essential aspects of natural ferritin.[10] We show that the sol−gel acts as a chemically active structure-directing agent to sequester iron atoms and promote the growth of superparamagnetic (blocking temperatures 8−12 K) iron−oxo nanoparticles (4−7 nm diameter) within its porous structure. A particularly remarkable feature of these gels is their ability to sequester iron under overload conditions and then release them into aqueous solution in the combined presence of reducing and chelating agents.

Sol−gels are framework polysiloxanes obtained by hydrolysis of alkoxysilane precursors.[12] The gels used in this study are prepared from an organically modified bis-[3-(trimethoxysilyl)-propyl]ethylenediamine (enTMOS) precursor $(CH_3O)_3Si(CH_2)_3$-$NH(CH_2)_2NH(CH_2)_3Si(OCH_3)_3$

Hydrolysis of this precursor forms an organic−inorganic hybrid material which contains both the organic component and the inorganic siloxane network.[11] The overall design strategy for selecting the enTMOS precursor is based on several factors that offer unique advantages to facilitate controlled growth of iron−oxo clusters. First, the enTMOS precursor, with two nitrogen atoms per formula unit, provides ligating atoms to sequester iron atoms into the sol−gel. Second, the amino groups in the network provide a high internal pH for formation of Fe−O−Fe linkages from iron−aquo complexes. Third, the presence of organic residues imparts an overall hydrophobic character to the material and thereby limits extensive aggregation of hydrophilic iron oxide to facilitate formation of smaller clusters. Finally, the nanometer-sized pores (∼4−7 nm) provide an ideal physical cavity for controlled growth of iron−oxo nanoparticles. Indeed, as we show in this work, the approach is quite effective for the formation of nanoparticles with 4−7 nm diameters.[13]

The morphology of the iron−oxo samples (labeled Fe1 to Fe7) was characterized by microscopy measurements. Figure 1 shows a typical TEM micrograph for sample Fe6. It is observed that the particles are spatially isolated from each other with a majority of particles having average diameters between 4 and 7 nm.

The magnetic properties of the samples were studied by a SQUID magnetometer in the range 2−300 K and up to 55 kOe in field cooling (FC) and zero field cooling (ZFC) experiments. Figure 2 shows the thermal variations of the ZFC magnetization (M(T)) at 100 Oe. The blocking temperature T_B (i.e., the temperature below which the spins are blocked by magnetic anisotropy) can be clearly determined by a maximum of $M(T)$ at low temperatures. The magnetization of Fe2 sample increases with decreasing temperature in a field of 100 Oe (Figure 2), however, a maximum can be detected in the low magnetic field of 40 Oe (Figure 2, inset). All of the samples exhibit blocking temperatures in the range 8−12 K. It is important to note that these values are in striking agreement with the blocking temperatures of 11−13 K reported for ferritin.[14,15] All of the samples studied in this work demonstrate superparamagnetic behavior, as indicated by temperature dependence of effective magnetic moment (μ_{eff}) which goes to zero at low temperature, suggesting an antiferromagnetic ground state (data not shown). We did not observe any anomalies on the $M(T,H)$ curves that could be related to the onset of any long-range interparticle interactions which is consistent with the fact that the particles are spatially isolated by the matrix.

The properties of the iron−oxo clusters investigated in this study are shown in Table 1. The overall results indicate that the number of iron atoms in these particles varies from 700 to 4000.[16] In general, there is a good agreement between the theoretically calculated blocking temperatures[17] and the experimentally observed values. Moreover, magnetic moments per cluster range from 100 to 2700 Bohr magnetons (BM). The significance of these values is particularly underscored when compared with the reported values for natural ferritin (300−400 μ_B)[18] and magnetoferritin (13200 μ_B).[19] Thus, the results indicate a considerable degree of similarity between the magnetic properties of iron−oxo samples and ferritin.

An additional remarkable feature of natural ferritin is its ability to sequester iron from external environment to form the iron−oxo core.[1] We evaluated the ability of enTMOS-derived samples to accumulate Fe^{3+} ions by making use of the changes in absorption intensity that occur in the 400-nm region due to formation of iron−oxo particles. Figure 3a shows the changes in

* To whom correspondence should be addressed.
[†] Department of Chemistry and Biochemistry.
[‡] Department of Physics.

(1) Harrison, P. M.; Arosio, P. *Biochim. Biophys. Acta* **1996**, *1275*, 161.
(2) Ziolo, R. F.; Giannelis, E. P.; Weinstein, B. A.; O'Horo, M. P.; Ganguly, B. N.; Mehrotra, V.; Russell, M. W.; Huffman, D. R. *Science* **1992**, *257*, 219.
(3) (a) Mann, S.; Hannington, J. P.; Williams, R. J. P. *Nature* **1986**, *324*, 565. (b) Kang, Y. S.; Risbud, S.; Rabolt, J. F.; Stroeve, P. *Chem. Mater.* **1996**, *8*, 2209.
(4) Mann, S. *Nature* **1993**, *365*, 499.
(5) Yaacob, I. I.; Nunes, A. C.; Bose, A. *J. Colloid Interface Sci.* **1995**, *171*, 73.
(6) Cannas, C.; Gatteschi, D.; Musinu, A.; Piccaluga, G.; Sangregorio, C. *J. Phys. Chem. B* **1998**, *102*, 7721.
(7) Li, S.; John, V. T.; Rachakonda, S. H.; Irvin, G. C.; McPherson, G. L.; O'Connor, C. J. *J. Appl. Phys.* **1999**, *85*, 5178.
(8) del Monte, F.; Morales, M. P.; Levy, D.; Fernandez, A.; Ocana, M.; Roig, A.; Molins, E.; O'Grady, K.; Serna, C. J. *Langmuir* **1997**, *13*, 3627.
(9) Lawson, D. M.; Artymuik, P. J.; Yewdall, S. J.; Smith, J. M. A.; Livingstone, J. C.; Treffry, A.; Luzzago, A.; Levi, S.; Arosio, P.; Cesareni, G.; Thomas, C. D.; Shaw, W. V.; Harrison, P. M. *Nature* **1991**, *349*, 541.
(10) Chasteen, N. D.; Harrison, P. M. *J. Struct. Biol.* **1999**, *126*, 182.
(11) Rao, M. S.; Dave, B. C. *J. Am. Chem. Soc.* **1998**, *120*, 13270.
(12) Brinker, C. J.; Scherer, G. *Sol-Gel Science: The Physics and Chemistry of Sol-Gel Processing*; Academic Press: Boston, 1990.
(13) The sol−gels were prepared by sonicating a mixture of 1.5 mL precursor, 0.4 mL of water, and 7.0 mL of methanol for 20 min. The resultant sol was poured in a polystyrene beaker and covered with Parafilm for 24 h. Monolithic sol−gels (diameter 25 mm, thickness 5 mm) were then immersed in 25 mL solution of ferric nitrate with varying concentrations (0.01 M, 0.025 M, 0.05M, 0.075, 0.1, 0.25, and 0.5 M) for 24 h.
(14) Tejada, J.; Zhang, X. X.; del Barco, E.; Hernandez, J. M.; Chudnovsky, E. M. *Phys. Rev. Lett.* **1997**, *79*, 1754.
(15) Gider, S.; Awschalom, D. D.; Douglas, T.; Mann, S.; Chaprala, M. *Science* **1995**, *268*, 77.
(16) Harrison, P. M.; Fischbach, F. A.; Hoy, T. G.; Haggis, G. H. *Nature* **1967**, *216*, 1188.
(17) Frankel, R. B.; Papaefthymiou, G. C.; Watt, G. D. *Hyperfine Interact.* **1991**, *66*, 71.
(18) Brooks, R. A.; Vymazal, J.; Goldfarb, R. B.; Bulte, J. W. W.; Aisen, P. *Magn. Res. Med.* **1998**, *40*, 227.
(19) Bulte, J. W. W.; Douglas, T.; Mann, S.; Frankel, R. B.; Loskowitz, B. M.; Brooks, R. A.; Baumgarner, C. D.; Vymazal, J.; Strub, M.-P.; Frank, J. A. *J. Magn. Reson. Imag.* **1994**, *4*, 497.

10.1021/ja003229n CCC: $20.00
Published on Web 01/26/2001

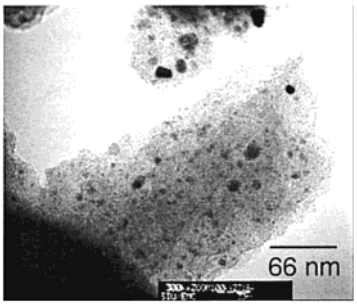

Figure 1. Transmission electron micrograph of Fe6 sample showing spatially isolated iron−oxo clusters in enTMOS sol−gels.

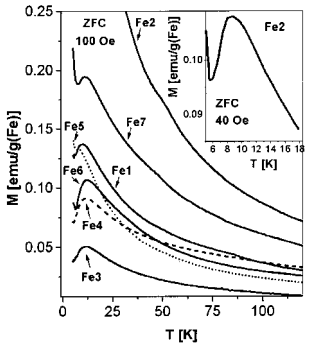

Figure 2. Variation in magnetization with respect to temperature for the iron−oxo samples in a magnetic field of 100 Oe after cooling in zero field (ZFC). The Fe2 sample does not show any maximum in the magnetic field of 100 Oe but a maximum can be seen at 40 Oe (inset).

Table 1. Properties of Iron−Oxo Clusters in enTMOS Sol−Gels

sample	average diameter[a] (nm)	Fe atoms/ cluster[b]	Fe atoms/ (g) sample[c]	blocking temp T_B (exp.)	blocking temp T_B (calc.)[d]	magnetic moment/ Fe (BM)	magnetic moment/ cluster (BM)
Fe 1	3.8	679	1.56×10^{21}	11.9	11.8	0.1981	134
Fe 2	4.7	1262	3.50×10^{21}	8.0	14.2	0.4214	532
Fe 3	5.0	1527	1.82×10^{21}	10.9	14.7	0.0662	101
Fe 4	5.1	1639	4.00×10^{21}	11.7	14.8	0.1500	246
Fe 5	5.3	1889	1.93×10^{21}	7.7	15.0	0.2792	527
Fe 6	5.6	2190	1.36×10^{21}	12.0	14.9	0.1661	364
Fe 7	6.6	4315	2.12×10^{21}	10.9	10.4	0.6248	2696

[a] From TEM. [b] Assuming a ferrihydrite ($5Fe_2O_3 \cdot 9H_2O$) unit cell (ref 16). [c] From atomic emission spectroscopy. [d] Using numerical methods described in ref 17.

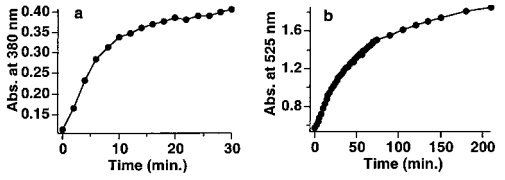

Figure 3. Intake and release of iron by 0.15 mm thick enTMOS films deposited on a glass substrate. (a) Intake of iron from a 0.01 M solution of ferric nitrate. (b) Release of iron from enTMOS film in the presence of sodium dithionite (0.1 mM) and 2,2′-bipyridine (0.5 mM).

absorbance at 380 nm when a film of pristine enTMOS sol−gel (glass slide substrate, thickness 0.15 mm) is exposed to a 0.01 M solution of Fe^{3+} ions. The growth of particles is rapid, and saturation is observed after 25 min. The rather exponential growth indicates an initial formation of template sites upon which subsequent buildup of further nuclei occurs. Thus, it appears that initially there is considerable free volume available and the growth of particles is faster. As the available space diminishes, the rate achieves saturation.

The natural ferritin also has the ability to release iron under reducing conditions in the presence of chelators to from apoferritin,[1] and we evaluated the ability of enTMOS materials to release iron under similar conditions. As shown in Figure 3b, the iron

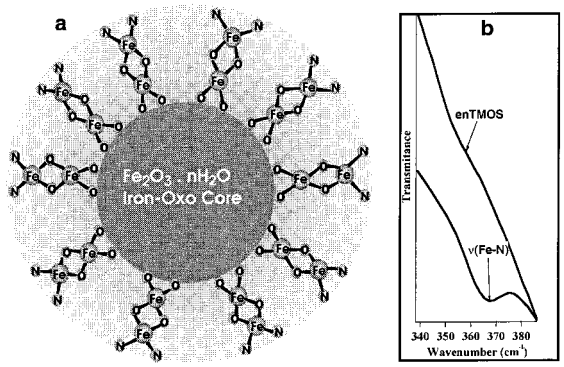

Figure 4. (a) Schematic two-dimensional representation of matrix-assisted assembly of iron−oxo clusters inside enTMOS sol−gel pores. (b) FTIR spectra of enTMOS gels with and without the iron−oxo clusters showing the appearance of ν(Fe−N) vibrational mode at 367 cm^{-1} in the sample containing the nanoclusters due to binding of metal ions to the amino groups of the sol−gel network.

atoms from the enTMOS sol−gels can be released into an external solution containing sodium dithionite and 2,2′-bipyridine (bpy). The release process was monitored by measuring the changes in absorbance at 525 nm. The release of iron atoms is slow and tends to saturate slowly after ∼3 h. It is important to note that the release profile is quite analogous to that reported for natural ferritin.[20] Also, we find that iron is not released when the sol−gels are placed in water or a solution of bpy. That is, both dithionite and bpy must be present for the release process to occur.

The exponential growth and release of the nanoclusters indicates a presence of cooperative processes that are convergent in nature. When placed in an aqueous solution of ferric salts, the enTMOS gels preferentially sequester iron atoms inside the porous network. This process is facilitated by amino groups which bind to the metal ions (Figure 4a), as confirmed by the appearance of a new peak corresponding to Fe−N stretching vibrational mode (Figure 4b). On the basis of the data, it appears that during the formation of the iron−oxo clusters: (a) initial iron atoms are bound to the pore walls of the sol−gel matrix through amino groups, (b) subsequent growth of the clusters occurs toward the center of the pore as more incoming iron atoms form oxo (or hydroxo)-bridged centers from iron aquo complexes,[21] and (c) the particle growth stops when the available volume within the pore is completely utilized (Figure 4a). Thus, taken together, the formation of clusters in enTMOS sol−gels is matrix-assisted and that the chemically active pores of the enTMOS sol−gel act as structure-directing agents for assembly of iron−oxo particles. This mechanism is also supported by the iron-release experiments. The initial faster rate of release indicates that the iron atoms from the center of the cluster are released first. After depletion of the central iron−oxo core, the rate of release is impeded due to competitive binding interaction of the iron atoms between the matrix and the chelating agent, causing a slow release of iron.

In conclusion, we have demonstrated biomimetic assembly of iron−oxo clusters in enTMOS sol−gels as synthetic analogues of ferritin. The assembly of these particles is assisted by the sol−gel matrix via formation of coordination bonds with the framework, and the system is able to mimic all of the essential aspects of natural ferritin. Finally, we note that these materials will find useful technological applications as transparent magnetic materials, as contrast agents for magnetic imaging, and as materials for magnetically targeted drug delivery.

Acknowledgment. This work was supported by grants from the Materials Technology Center at SIU (B.C.D.) and CARS-University of Chicago (N.A. and B.C.D.). We thank Professor V. M. Malhotra for assistance with FTIR measurements.

JA003229N

(20) Courteix, A.; Bergel, A. *AIChE J.* **1996**, *42*, 829.
(21) Flynn, Jr, C. M. *Chem. Rev.* **1984**, *84*, 31.